The Hyperbolic Tangent World

L. David Roper
http://roperld.com/personal/RoperLDavid.htm
This is web page http://www.roperld.com/science/HyperbolicTangentWorld.pdf

Contents

Chapter 1. Introduction

At first glance it may appear to be a mystery as to why so many of the events of the Universe can be modeled with mathematics. Some have declared that the Universe is just a super-giant computer which, of course, uses mathematics to do its calculations. (**Arianrhod, 2003**)

This article deals with a sub-mystery of the mathematics mystery in trying to explain why so many events of the Universe can be modeled to varying degrees of accuracy by the simple mathematics function, the hyperbolic tangent, whose definition (http://en.wikipedia.org/wiki/Hyperbolic_tangent) is

$$\tanh(x) = \tanh x = \frac{e^x - e^{-x}}{e^x + e^{-x}}. \tag{1.1}$$

(e is the irrational number 2.71828183….
See http://en.wikipedia.org/wiki/Exponential_function.) Figure 1-1 is a graph of the hyperbolic tangent.

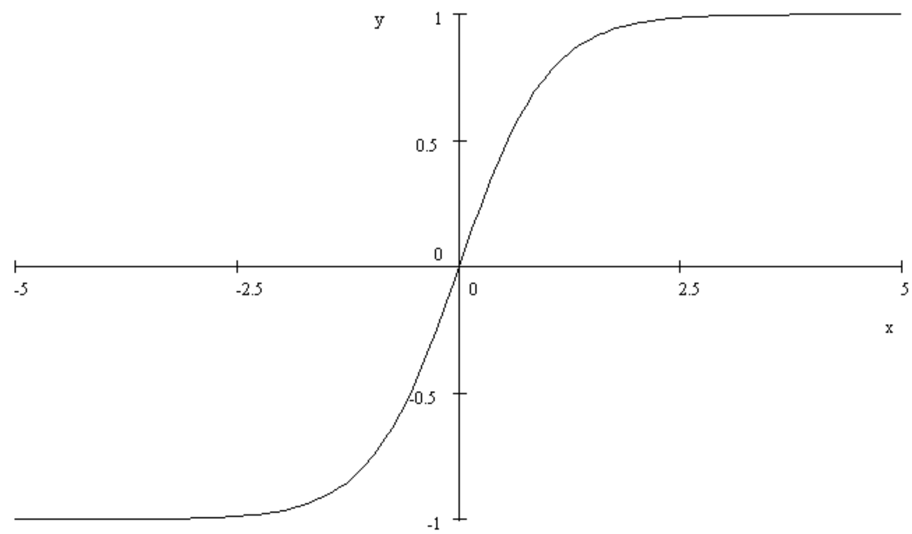

Figure 1-1. The hyperbolic-tangent function.

The hyperbolic-tangent has interesting asymptotic properties:

$$\tanh(x)=\frac{e^x-e^{-x}}{e^x+e^{-x}}\begin{cases}\xrightarrow[x\to-\infty]{}-1\\ \xrightarrow[0>x\gg-1]{}e^{2x}-1\\ \xrightarrow[x\to 0]{}0\\ \xrightarrow[0<x\ll+1]{}e^{2x}-1\\ \xrightarrow[x\to+\infty]{}+1\end{cases}. \tag{1.2}$$

Figure 1-2 shows the hyperbolic tangent and the $\left(e^{2x}-1\right)$ function plotted together.

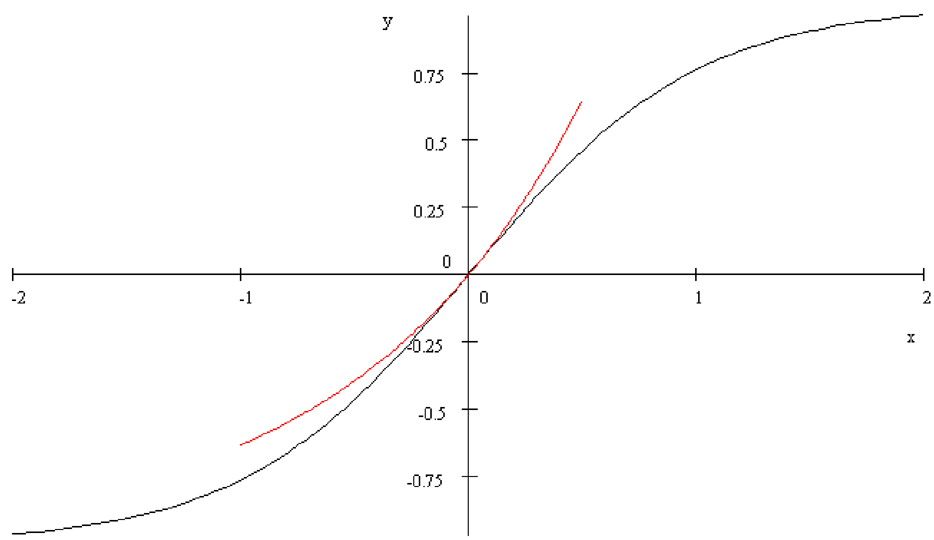

Figure 1-2. The hyperbolic-tangent function and the $\exp(x)-1$ function.

The following holds:

$$\frac{1}{2}\left[1+\tanh\left(x\right)\right]=\frac{e^{x}}{e^{x}+e^{-x}}\begin{cases}\xrightarrow[x\to-\infty]{}0\\ \xrightarrow[x\ll-1]{}\frac{1}{2}e^{2x}\\ \xrightarrow[x\to0]{}\frac{1}{2}\\ \xrightarrow[x\to\ll+1]{}\frac{1}{2}e^{2x}\\ \xrightarrow[x\to+\infty]{}+1\end{cases}. \tag{1.3}$$

This function is graphed in Figure 1-3.

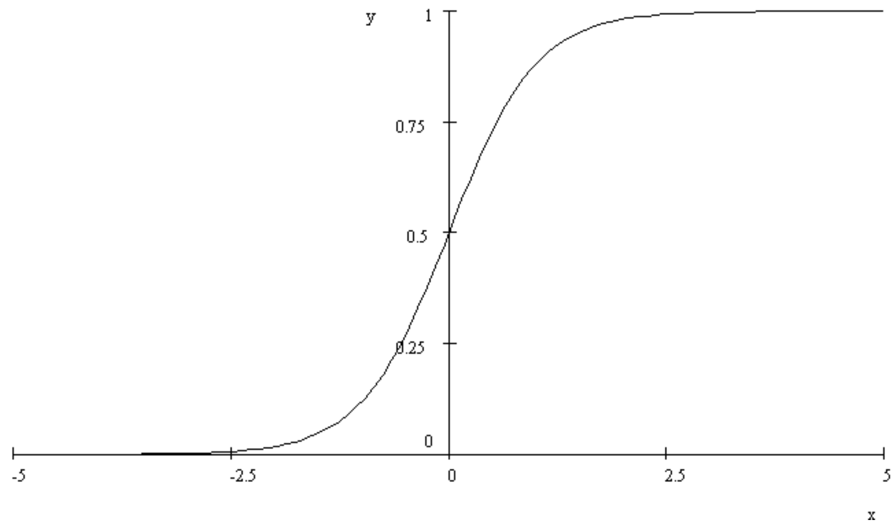

Figure 1-3 The $\frac{1}{2}\left[1+\tanh\left(x\right)\right]$ **function.**

Note that the function of Eq. (1.3) has the very nice property of being zero for large negative x and 1 for large positive, having gone through zero at x = zero. One can multiply this function by any number to model many natural phenomena which start at zero for some parameter 1 for a large negative value of parameter 2 and then exponentially rise near zero for parameter 2 and then asymptotically approach the multiplying constant for parameter 1 at large parameter 2.

A more general function is needed for real-World fits to natural phenomena, as given in the following equation.

$$Q\left(x;C,p,w\right)=\frac{C}{2}\left[1+\tanh\left(\frac{x-p}{2w}\right)\right] \tag{1.4}$$

For example, $\frac{1}{2}\left[1+\tanh\left(\frac{x-2}{5}\right)\right]$ is plotted in Figure 1-4.

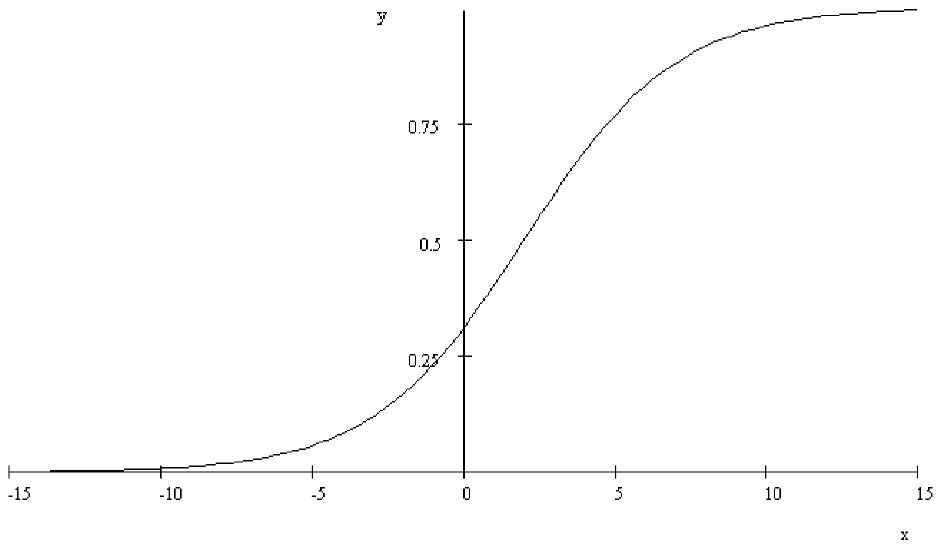

Figure 1-4. Plot of $\frac{1}{2}\left[1+\tanh\left(\frac{x-2}{5}\right)\right]$**.**

We see why the parameter symbols w and p were chosen in the more general hyperbolic tangent in Eq. (1.3) when we take the derivative of the function.

$$\frac{d}{dx}\left\{\frac{C}{2}\left[1+\tanh\left(\frac{x-p}{2w}\right)\right]\right\}=\frac{C}{4w}\left[1-\tanh^2\left(\frac{x-p}{2w}\right)\right]=P\left(x;C,p,w\right). \tag{1.5}$$

Figure 1-5 is a plot of $\frac{1}{2\bullet 5}\left[1-\tanh^2\left(\frac{x-2}{5}\right)\right]$.

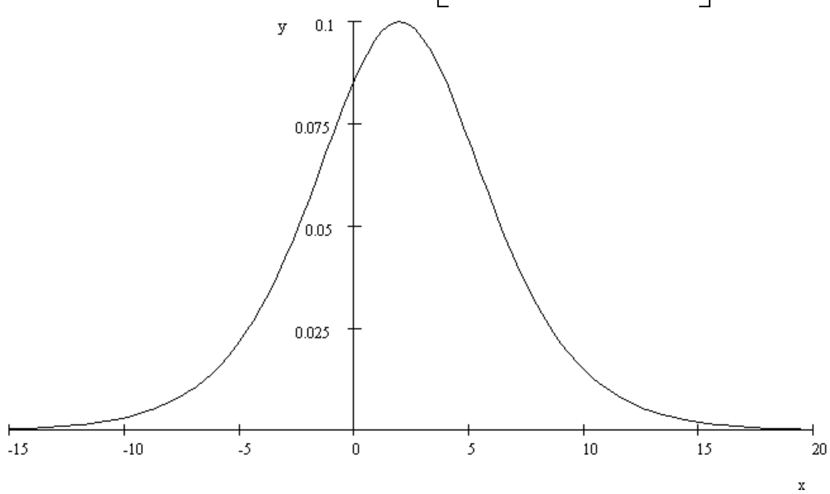

Figure 1-5. Plot of $\frac{1}{2\bullet 5}\left[1-\tanh^2\left(\frac{x-2}{5}\right)\right]$**.**

The equation's parameters have the following meanings:

$$
\begin{aligned}
&p = \text{peak position of the function}\\
&w = \text{ a measure of the width of the function; also the exponential time constant near } x = p\\
&\frac{C}{4w} = \text{height of the function}
\end{aligned}
\tag{1.6}
$$

Sometimes natural data are in the form of an asymptotic curve such as Eq. (1.4) and sometimes natural data are in the form of a peaked curve, such as Eq. (1.5). As shown above, they are related by a calculus derivative, or inversely a calculus integral.

For minerals depletion (**Roper, 1976**) the relevant equations are

$$
\begin{aligned}
&Q(t;C,p,w) = \frac{C}{2}\left[1-\tanh\left(\frac{t-p}{2w}\right)\right] = \text{amount yet to be extracted at time } t\\
&\text{and } P(t;C,p,w) = -\frac{dQ}{dt} = \frac{C}{4w}\left[1-\tanh^2\left(\frac{t-p}{2w}\right)\right] = \text{the extraction rate.}
\end{aligned}
\tag{1.7}
$$

It is rare that natural peaked data are symmetrical about the peak; similarly asymptotic data often have a different rate going into the asymptote than the growth rate from zero. One needs a generalization of the hyperbolic tangent that allows such asymmetry. Such a generalization, the Verhulst function, is derived in (**Roper, 1976)**.

$$
Q(t;C,p,w) = \frac{Q_\infty}{\left[1+\left(2^n-1\right)\exp\left\{\frac{t-p}{w}\right\}\right]^{\frac{1}{n}}} \text{ and } P(t;C,p,w) = \frac{Q_\infty}{nw}\frac{\left(2^n-1\right)\exp\left\{\frac{t-p}{w}\right\}}{\left[1+\left(2^n-1\right)\exp\left\{\frac{t-p}{w}\right\}\right]^{\frac{n+1}{n}}}. \tag{1.8}
$$

For $n=1$ Eq.(1.8) reduces to Eq. (1.7), the symmetric case. For $0 \geq n \geq 1$ skewing is toward short times and for $n<1$ skewing is toward large times.

Now that we have seen the mathematical shape of the hyperbolic tangent it is not so mysterious why it is applicable to so many physical processes. Many physical processes have several different states of existence. The hyperbolic tangent is a function that can easily represent the transition from one state to another.

For turning on and then off a state the following function works quite well:

$$\frac{c}{2}\left[\tanh\left(\frac{t-t_i}{w_i}\right)-\tanh\left(\frac{t-t_o}{w_o}\right)\right], \text{ where}$$

t_i = transition time position for going into the state and

t_o = transition time position for leaving the state;

w_i = width for going into the state and

w_o = width for leaving the state.

For example, Figure 1-6 shows the two transitions represented by $\frac{1}{2}\left[\tanh\left(\frac{t-2}{0.5}\right)-\tanh\left(\frac{t-10}{1}\right)\right]$.

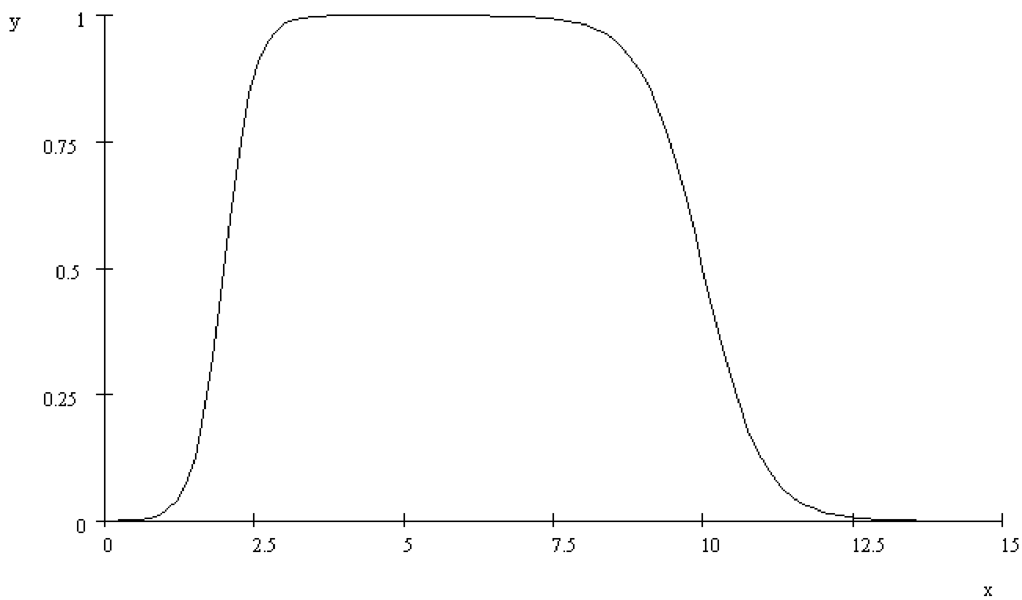

Figure 1-6. Plot of $\frac{1}{2}\left[\tanh\left(\frac{t-2}{0.5}\right)-\tanh\left(\frac{t-10}{1}\right)\right]$

Chapter 2. World Population

It appears that World population growth is beginning to decline. The ideal situation would be that it would approach an asymptote rather than continuing to grow exponentially or disastrously decline by terrible calamities. A Verhulst function can be fitted to the data since 1950 to yield the curves shown in Figure 2-1.

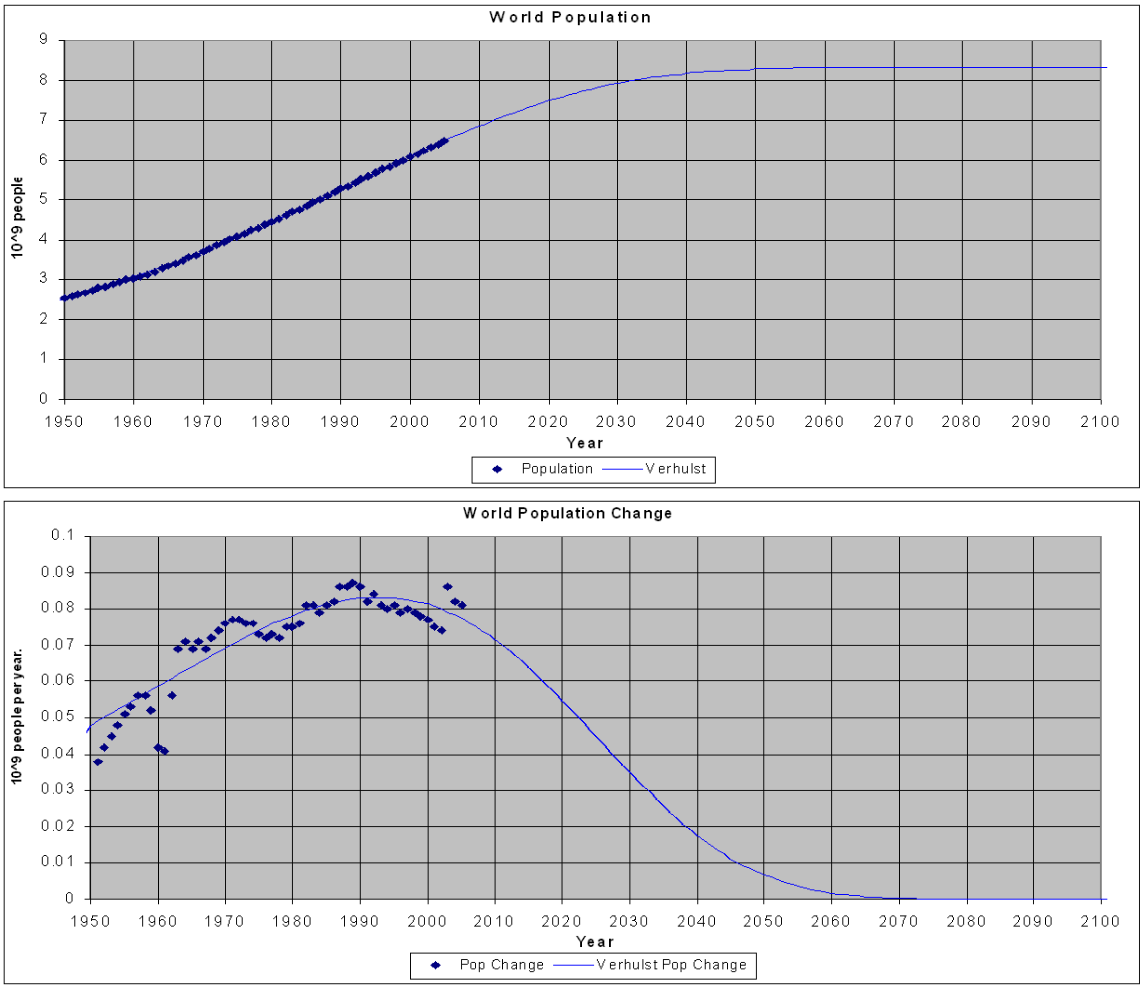

Figure 2-1. A Verhulst function fit to the World population data from 1950. Top: The population data. Bottom: The change in population.

For a more detailed analysis of World population see (**Roper, 1977**).

Chapter 3. Crude Oil Depletion in the United States and the World

Crude Oil Extraction in the United States

The rate of crude oil extraction ("extraction", not "production"!) in the United States is shown in Figure 3-1.(**Heinberg, 2003**) It peaked about 1970, got a slight boost from Alaska extraction in the 1980s, but has declined steadily for the last twenty years and will continue to do so with possible short-lived small peaks. The Verhulst function fit (**Roper, 1976**) to the data gives a reserves value 1.5 times the 2003 proven reserves, which probably is about right for predicting the future.

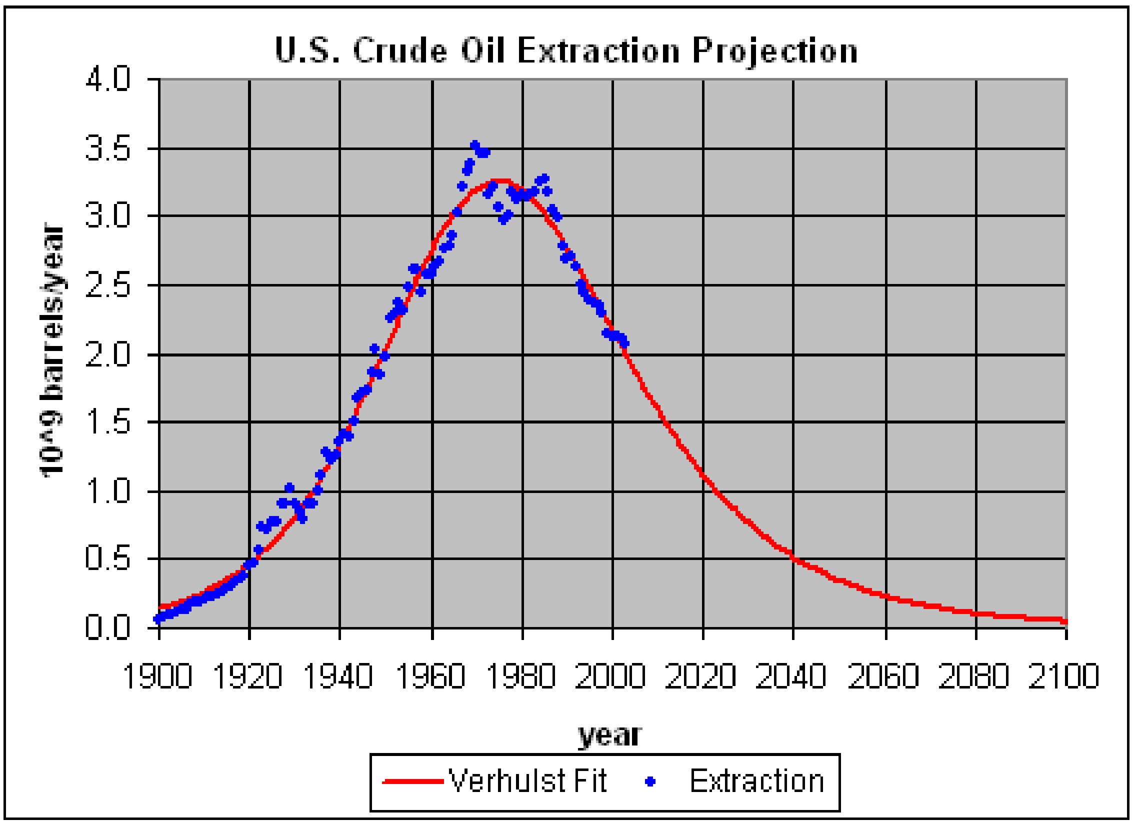

Figure 3-1. United States extraction rate of crude oil, a fit using the Verhulst function and the fit's projection into the future. Data are from http://www.eia.doe.gov .

Note that the extraction curve is not symmetrical; it is skewed toward future times. This is to be expected as Herculean efforts will be made to extract crude oil in the future.

Crude Oil Extraction for the World

Figure 3-2 shows crude oil discoveries rate. Note the peak in discoveries at about 1965 and the rapid fall since about 1975. The Verhulst function fit (**Roper, 1976**) to the discoveries data gives the total amount of crude oil to be extracted as slightly less than 2 x 10^{12} (2 trillion) barrels. Obviously, World crude oil discoveries have been meager and declining for the last thirty years.

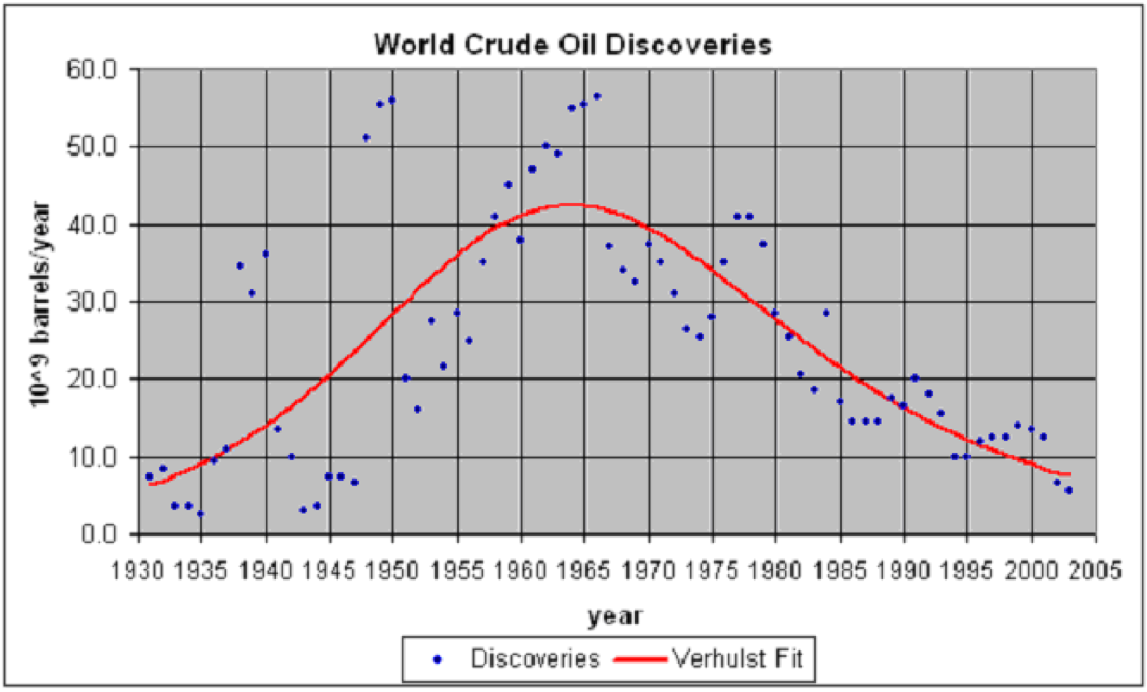

Figure 3-2. World crude oil discoveries rate and a Verhulst-function fit to the data. Data are from http://www.durangobill.com/Rollover.html .

Extraction rates for crude oil are typically about forty years behind discoveries rates. So, the World crude oil extraction rate is expected to peak at about 2005.

Figure 3-3 shows the World crude oil extraction rate and two mathematical fits to the data. The two Verhulst function fits (**Roper, 1976**) were obtained by fixing the total amount of World crude oil to be extracted at 2×10^{12} (2 trillion) barrels, an amount consistent with the fit to World crude oil discoveries discussed above and shown in Figure 3-3 and at 3×10^{12} barrels, 50% more than the amount that fits the discoveries rate data.

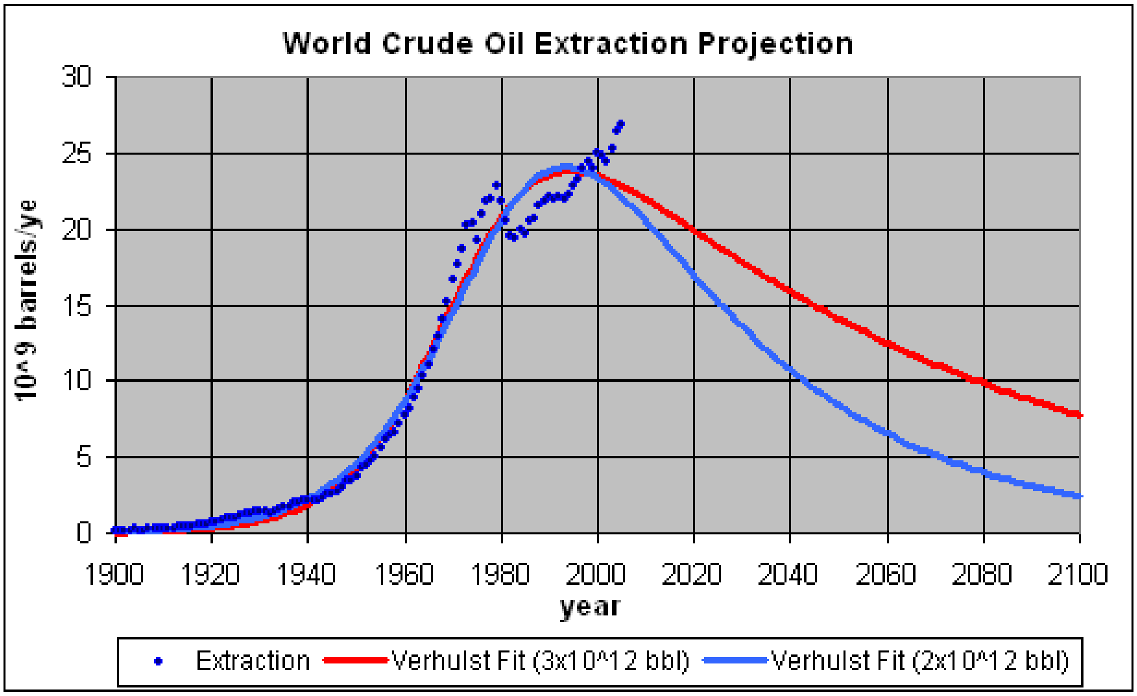

Figure 3-3. World crude oil extraction rate, two fits using the Verhulst function and projection of the fits into the future. Data are from http://www.eia.doe.gov .

The peak has been predicted by many geologists to be between 2000 and 2010. (**Deffeyes, 2005**)

Whether the peak of crude oil extraction has already occurred or will occur in the near future, the message is the same: The World, led by the United States, must use the remaining crude oil mostly to develop the infrastructure needed for the use of renewable energy sources beginning now and into the future.

For more information about crude oil depletion see (**Roper, 2005**) and (**Roper, 2006**).

Chapter 4. The Last Four Major Ice Ages

Ice cores from Vostok Antarctica have yielded temperature data for the last 422,000 years. In that period of time there were four Major Ice Ages of about 115,000 years duration each.

In (**Roper, 2004**) it is shown that those last four Major Ice Ages can be reasonably fitted with Earth states transitions represented by hyperbolic tangents. The mathematical equation used to make the fits is

$$T_I(t) = C + F \cdot I(t) + \sum_{i=1}^{N} \sum_{j=1}^{N_{MIA}+1} s_{ij} \frac{1}{2}\left[\tanh\left(\frac{t-\left(c_{1ij}+t_j\right)}{w_{1ij}}\right) - \tanh\left(\frac{t-\left(c_{2ij}+t_j\right)}{w_{2ij}}\right)\right]$$

$=$ temperature in degrees C, where $I(t) =$ calculated North-Pole insolation at time t,

$t_j =$ time of the j$^{\text{th}}$ Major Interglacial relative to now.

Double-sigmoid parameters: $s_{ij} =$ strength, $c_{nij} =$ position, $w_{nij} =$ width.

$N =$ number of double sigmoids used in the fit.

$N_{MIA} =$ number of Major Ice Ages to be fitted and predicted.

The fits to the last four Major Ice Ages and predictions for the next two Major Ice Ages are shown in Figure 4-1.

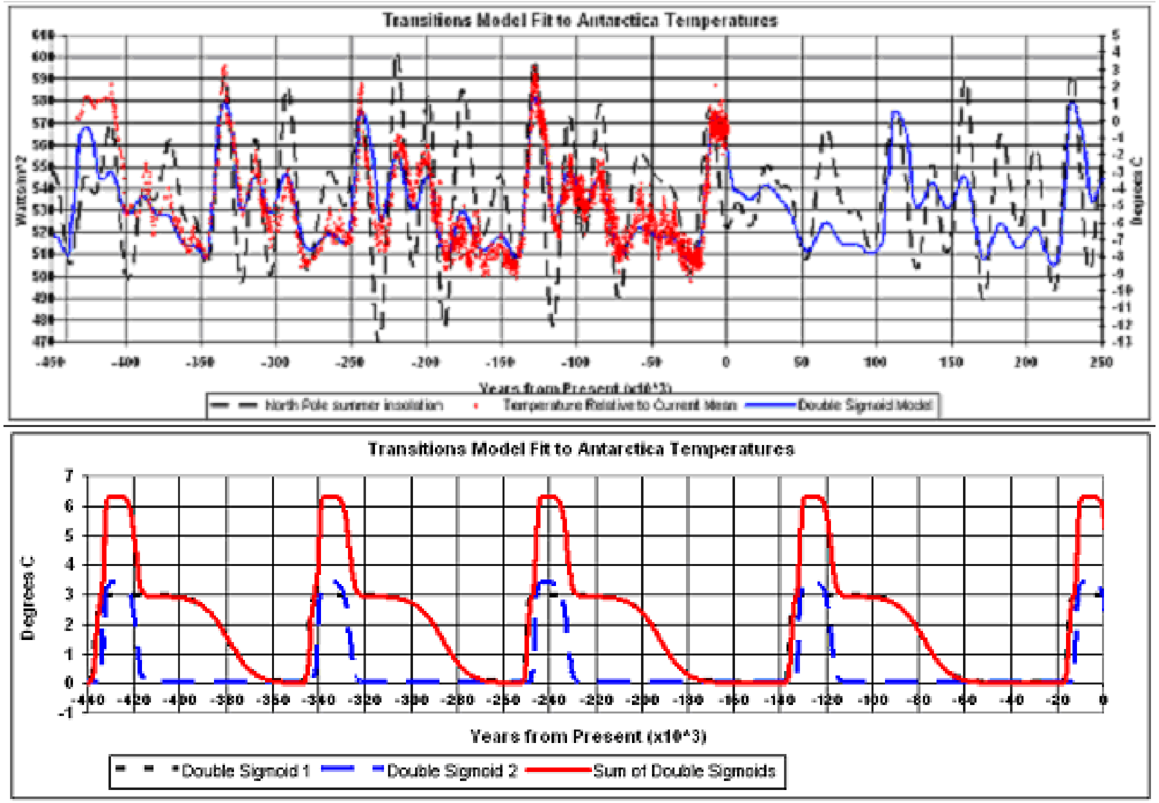

Figure 4-1. Fits to Antarctica temperature data for the last four Major Ice Ages by a

mathematical function involving the North-Pole summer insolation and two Earth states transitions in the time vicinity of the five Major Interglacials (Roper, 2004). The fit is then projected into the future for the next two Major Ice Ages. The bottom graph shows the two Earth states transitions and their sum (solid curve).

For more details see (**Roper, 2004**).

Chapter 5. Nerve Action Potential

The time dependence of the "action potential" across the excitable membrane of the axon of a nerve cell can be represented by a combination of several hyperbolic tangents. (See http://en.wikipedia.org/wiki/Action_potential, http://en.wikipedia.org/wiki/Membrane_potential, http://en.wikipedia.org/wiki/Nernst_equation, http://en.wikipedia.org/wiki/Axon, and http://en.wikipedia.org/wiki/Hodgkin-huxley_model .)

A typical action potential (inside relative to outside) is shown in Figure 5-1.

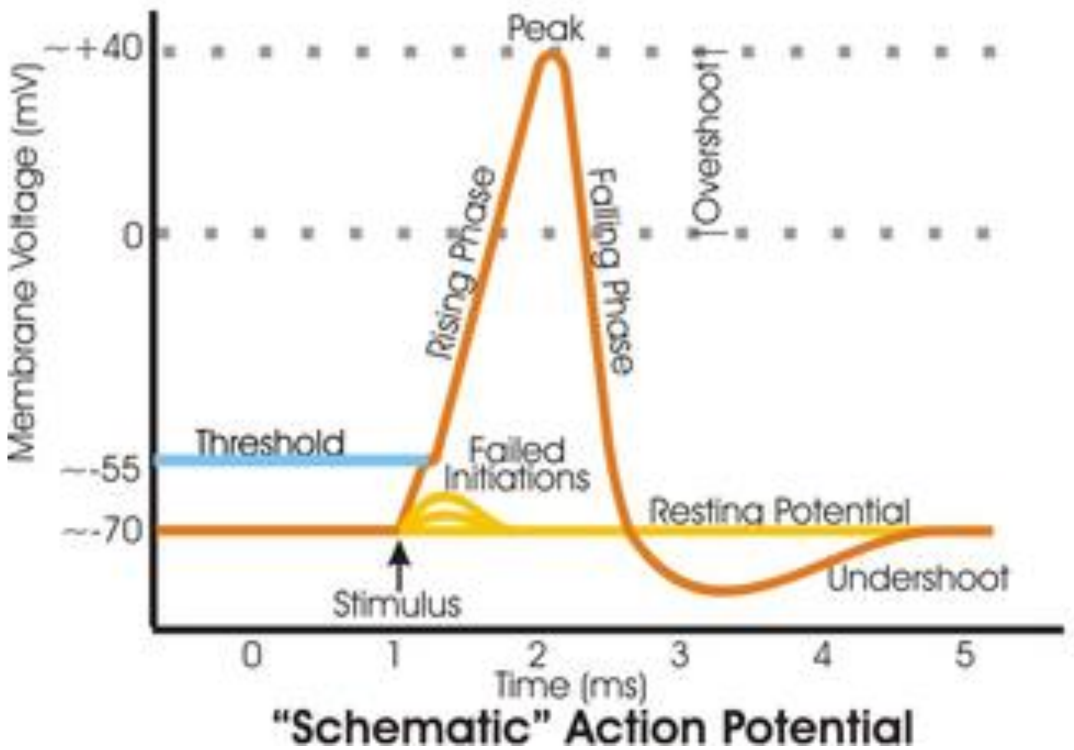

Figure 5-1. A typical nerve axon action potential (http://en.wikipedia.org/wiki/Action_potential).

The explanation for the action potential, which once generated travels down the nerve axon with a speed of 10 to 100 meters/second, is as follows:

- A resting electric potential of about -70 milliVolts (mV) inside relative to outside exists due to concentration differences across the squid giant axon lipid membrane as follows:
    - 400 millimoles/liter (mM/l) inside and 20 mM/l outside for K^+ ions.
    - 50 mM/l inside and 440 mM/l outside for Na^+ ions.
    - About 100 mM/l inside and 560 mM/l outside for Cl^- ions.
    - There are other ions present, such as Ca^{++}, with concentration gradients across the membrane.
    - The main cause of the -65-mV resting potential is that the membrane is mainly permeable to K^+ ions at rest, so that some K^+ ions migrate to the outside setting up the potential.
- An applied positive transient electric potential inside relative to outside above a threshold value (about 40 mV) triggers a brief opening of a channel that allows Na^+ ions to pass into the axon, causing the membrane potential to transiently move positively.
- That is followed by a brief opening of a channel that allows a greater flow of K^+ ions outside the axon, which typically causes an overshoot below the resting potential
- Eventually the membrane potential restores to the resting potential, unless the stimulating potential is maintained, in which case, after a refractory period, it is repeated.

The opening of the two ion channels can be represented mathematically by two double hyperbolic tangents:

$$V(t) = V_r + \frac{1}{2} C_{\mathrm{Na}} \left[\tanh\left(\frac{t - t_{\mathrm{Na1}}}{w_{\mathrm{Na1}}} \right) - \tanh\left(\frac{t - t_{\mathrm{Na2}}}{w_{\mathrm{Na2}}} \right) \right] + \frac{1}{2} C_{\mathrm{K}} \left[\tanh\left(\frac{t - t_{\mathrm{K1}}}{w_{\mathrm{K1}}} \right) - \tanh\left(\frac{t - t_{\mathrm{K2}}}{w_{\mathrm{K2}}} \right) \right],$$

where $V_r = \mathrm{K}^+$ resting potential.

An example of a calculated action potential is shown in Figure 5-2.

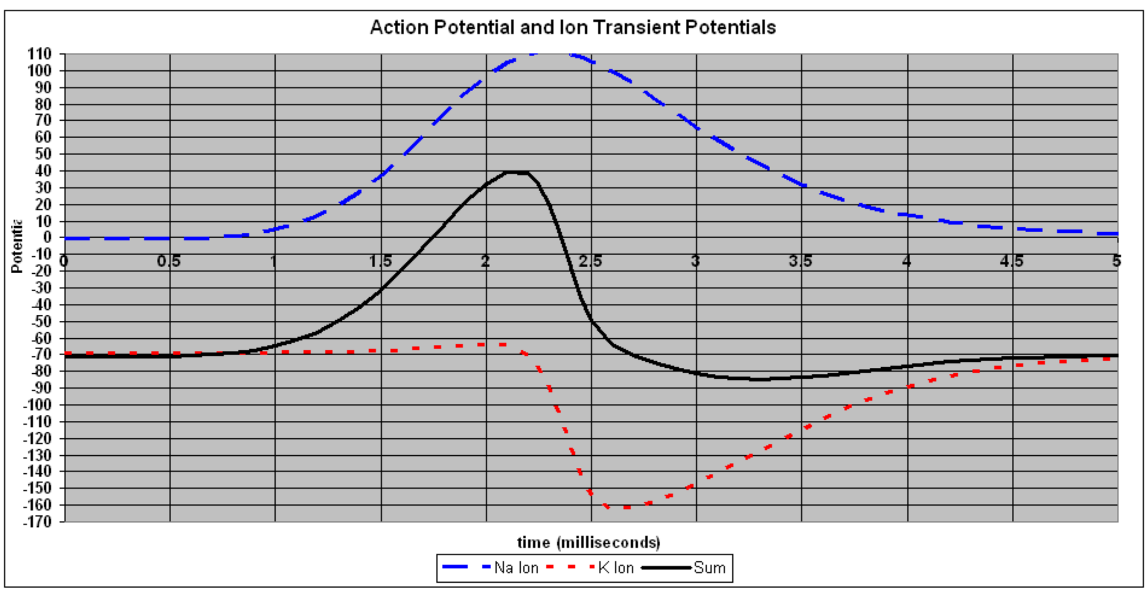

Figure 5-2. Example of a calculated action potential using two double hyperbolic tangents for the two ion channels. The two double hyperbolic tangents are shown along with the sum of them.

The parameters for this curve are:

$V_r = -70$	C	t_1	w_1	t_2	w_2
Na parameters:	264	1.82	0.625	2.50	1.02
K parameters:	-118	2.37	0.143	3.28	0.887

One can create many different shapes for action potentials by varying the ten parameters in the equation. Figure Figure 5-3 shows an example of a different shape.

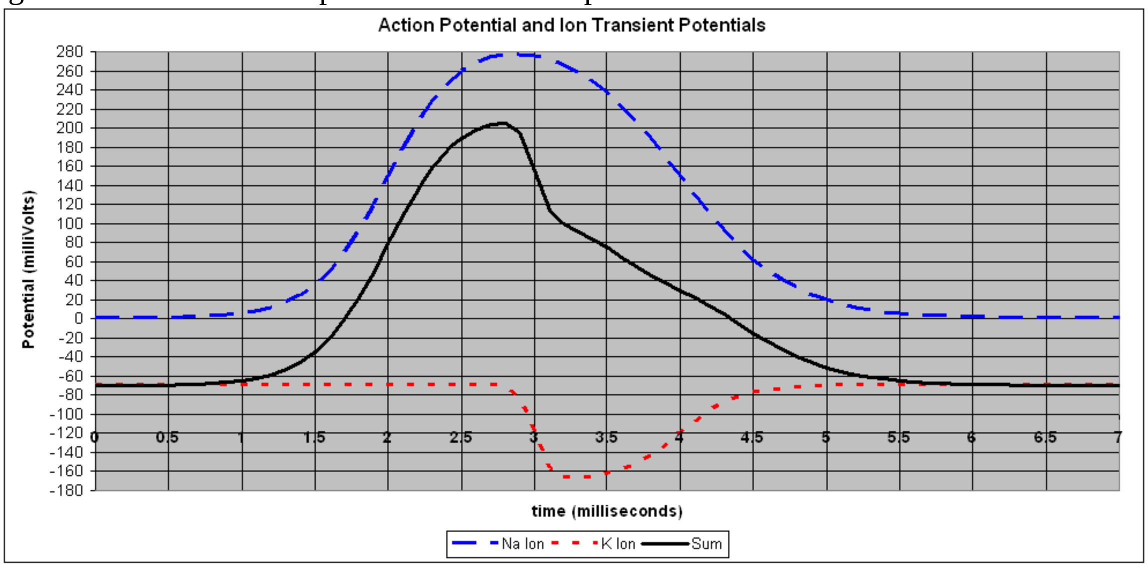

Figure 5-3. Example of a calculated action potential using two double hyperbolic tangents for the two ion channels. The two double hyperbolic tangents are shown along with the sum of them.

The parameters for this curve are:

$V_r = -70$	C	t_1	w_1	t_2	w_2
Na parameters:	300	2	0.5	4	0.75
K parameters:	100	3	0.1	4	0.4

These curves do not contain the transient stimulus electric potential of about +40 mV. It can be subtracted out from the measurement. It could be added to the equation as another double hyperbolic tangent.

If more ions are involved with channels opening, such as Ca^{++}, they can be added as another double hyperbolic tangent.

It would be interesting to try to obtain an approximation to the Hodgkin-Huxley equations (http://biolpc22.york.ac.uk/hh/hh_excel.html) for the action potential by mathematically manipulating the equation given here.

For details about fits to voltage-clamp data see http://www.roperld.com/science/NerveExcitation.pdf .

Chapter 6. Bush Iraq War Surges

The Bush Iraq War had two "surges" of United States troops involved from its beginning in March 2003 to the end of 2007. Those two surges are very well fitted by two hyperbolic tangent functions as shown in

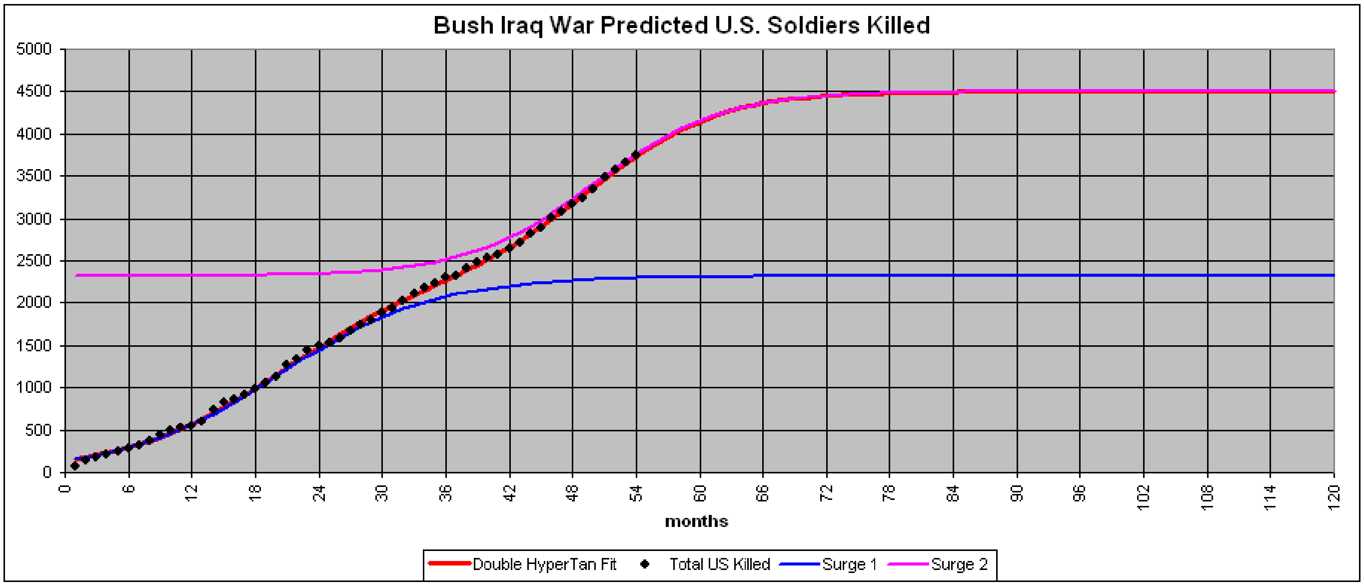

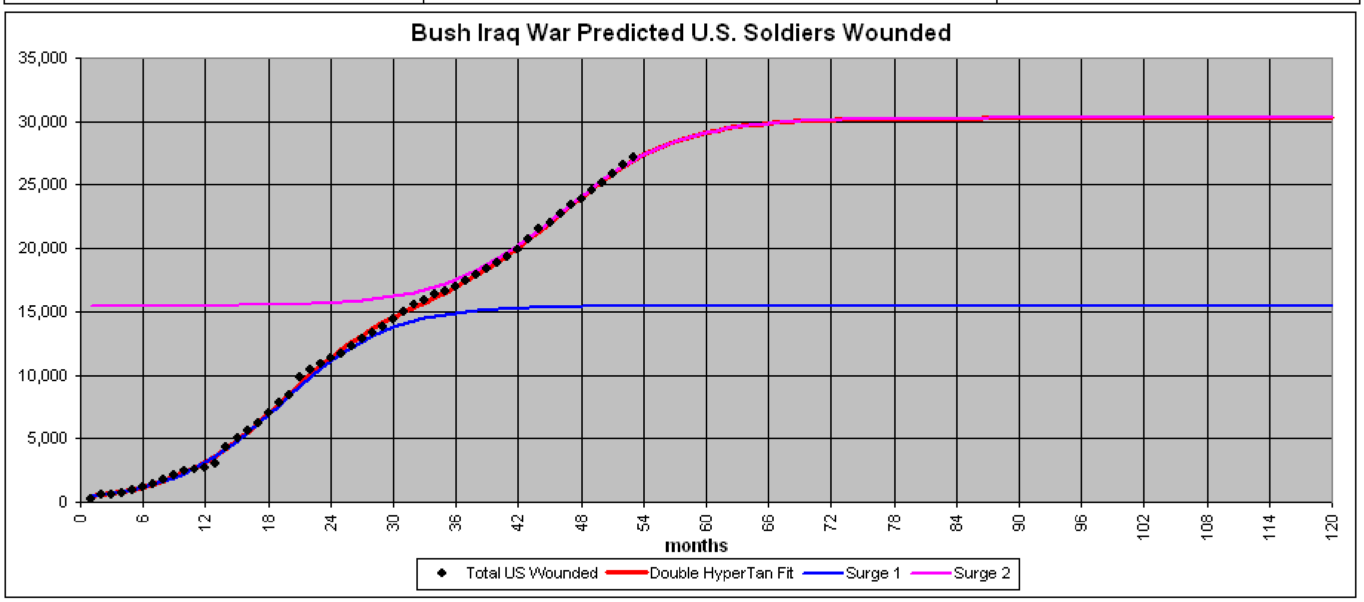

The parameters of the fit to the number killed are:

1. Surge 1: asymptote = 2321 killed, inflection point = 20.3 months, asymmetry parameter = 14.7
2. Surge 2: asymptote = 2184 killed, inflection point = 50.0 months, asymmetry parameter = 12.0

The parameters of the fit to the number wounded are:

3. Surge 1: asymptote = 15,456 killed, inflection point = 19.1 months, asymmetry parameter = 10.4
4. Surge 2: asymptote = 14,813 killed, inflection point = 46.1 months, asymmetry parameter = 11.1

References

- **Arianrhod, 2003**: *Einstein's Heroes*, Robyn Arianrhod, Univ. of Queensland Press, 2003.
- **Bartlett, 2004**: *The Essential Exponential: For the Future of Our Planet*, Albert A. Bartlett, Univ. of Nebraska, 2004.
- **Roper, 1976**: *Depletion Theory*, L. David Roper, http://arts.bev.net/RoperLDavid/minerals/DepletTh.pdf, 1976.
- **Roper, 1997:** *Projection of World Population*, L. David Roper, http://arts.bev.net/roperldavid/WorldPop.htm, 1997.
- **Roper, 2004**: Major Ice Ages Earth-States Transitions, L. David Roper, http://www.roperld.com/Science/TransitionsModelMIA.pdf, 2004.
- **Roper, 2005**: World and United States Crude Oil Depletion, L. David Roper, http://arts.bev.net/roperldavid/minerals/crudeoil.htm, 2005.
- **Roper, 2006**: Triple Threats for the Human Future: Will Civilization Arrive, L. David Roper, http://www.roperld.com/science/HumanFuture.pdf, 2006.
- **Roper, 2010**: http://roperld.com/science/minerals/VerhulstFunction.pdf
- **Roper, 2023**: http://roperld.com/science/MultiStatesMathematics.pdf

L. David Roper, http://roperld.com/personal/RoperLDavid.htm

See http://www.roperld.com/HumanFuture.htm

21 August 2006